

國立臺灣大學生命科學院基因體與系統生物學學位學程  
碩士論文

Genome and Systems Biology Program  
College of Life Sciences  
National Taiwan University  
Master's Thesis



酵母必需基因中 Hsp90 可緩衝突變的遺傳篩選

A genetic screen for Hsp90 bufferable mutants in yeast  
essential genes

林克文

Nicholas Francis Hoeffner

指導教授: 呂俊毅 博士 & 蔡懷寬 博士

Advisors: Jun-Yi Leu, PhD & Huai-Kuang Tsai, PhD

中華民國 112 年 8 月

August 2023

國立臺灣大學碩士學位論文  
口試委員會審定書  
MASTER'S THESIS ACCEPTANCE CERTIFICATE  
NATIONAL TAIWAN UNIVERSITY



(論文中文題目) (Chinese title of Master's thesis)


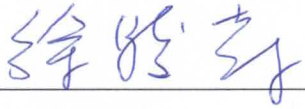

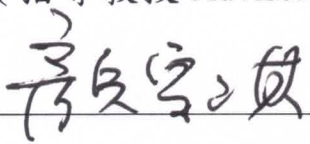

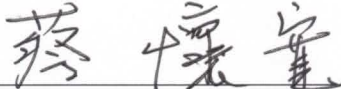
(論文英文題目) (English title of Master's thesis)

A Genetic Screen for Hsp90 Bufferable Mutants in  
Yeast Essential Genes

本論文係 Nicholas Hoeffner (姓名) r10b48009 (學號) 在國立臺灣大學  
GSB (系/所/學位學程) 完成之碩士學位論文，於民國 112 年  
7 月 20 日承下列考試委員審查通過及口試及格，特此證明。

The undersigned, appointed by the Department / Institute of GSB  
on 20 (date) 7 (month) 2023 (year) have examined a Master's thesis entitled above presented  
by Nicholas Hoeffner (name) r10b48009 (student ID) candidate and hereby certify  
that it is worthy of acceptance.

口試委員 Oral examination committee:

 (指導教授 Advisor)		
		
		

系主任/所長 Director: 鄭石通

## Acknowledgments



Throughout my studies I have been incredibly privileged to receive the support of so many around me. In particular, I owe so much to my partner Amber, whose hard work and patience afforded me the ability to work many long days and late nights. I would also like to thank her family for their support, generosity and inviting attitudes. I acknowledge that my choosing to do my master's studies on the opposite side of the globe was not the ideal decision for my parents and I am deeply grateful to them for their understanding and encouragement. The occasional chats I have had with my brother about my both my project and life in general have been truly valuable and therapeutic to me and I owe a large portion of my passion for science to him.

I feel very lucky to have been a member of N411 and I am constantly amazed at the intelligence and productivity of all of those around me. My peers in this lab have been invaluable in so many respects. From offering advice for troubleshooting experiments, to helping me to communicate with the administration at my university, to providing me with perspective about life, my colleagues have never hesitated to selflessly devote some time to me. Lastly, I would like to thank my advisor, Jun-Yi for all of his encouragement, guidance and for acting as a source of inspiration. The environment of our lab which has been so nurturing for me is no doubt the result of his careful cultivation.

Nick Hoeffner

# 酵母必需基因中 Hsp90 可緩衝突變的遺傳篩選

**Nick Hoeffner<sup>1,2</sup>, Jun-Yi Leu<sup>1,2</sup> and Huai-Kuang Tsai<sup>1,3</sup>**


<sup>1</sup>Genome and Systems Biology Degree Program, National Taiwan University

<sup>2</sup>Institute of Molecular Biology, Academia Sinica

<sup>3</sup>Institute of Information Science, Academia Sinica

## 摘要:

Hsp90 是一種分子伴侶蛋白，對大部分真核生物蛋白質組的數量有直接或間接的影響。過去觀察到 Hsp90 具有緩衝遺傳變異的能力，也就是說，它在細胞中的存在可以抵銷或減弱與基因變異或突變體相關聯的表現型強度。目前人們已提出了幾種機制來解釋這種現象，其中一些機制需要 Hsp90 的結合並穩定突變蛋白質，而其他機制則認為，由於 Hsp90 下游因子導致突變蛋白質的數量增加，使得該蛋白質能夠容忍其活性小幅度的降低。Hsp90 的緩衝能力在進化中可能扮演著重要角色，因為它決定了哪些變異體將有助於人口的表型多樣性以及在什麼條件下發揮作用。為了評估它們的影響力和性質，需要更好地了解受 Hsp90 緩衝的變異體的普遍性和特徵，以及主要的緩衝機制。在這篇論文中，我們利用偽尿嘧啶合成酶 CBF5 作為目標基因，創建並利用基因篩檢以識別在酵母基因中具有 Hsp90 緩衝作用的 CBF5 點突變。我們將由易錯聚



合酶鏈反應產生的 CBF5 突變基因庫轉化為條件性 CBF5 酵母抑制株，並通過 Tet-Off 啟動子來控制 Hsp90 的水平。我們在正常和降低 Hsp90 條件下對突變體的適應性進行測試，並鑒定出幾種具有 Hsp90 緩衝表現型的突變體。此外，我們還開發了一種基於複製板和影像分析以快速識別這些酵母菌落表現型的方法。

# A genetic screen for Hsp90-Bufferable mutants in yeast essential genes



**Nick Hoeffner<sup>1,2</sup>, Jun-Yi Leu<sup>1,2</sup> and Huai-Kuang Tsai<sup>1,3</sup>**

<sup>1</sup>Genome and Systems Biology Degree Program, National Taiwan University

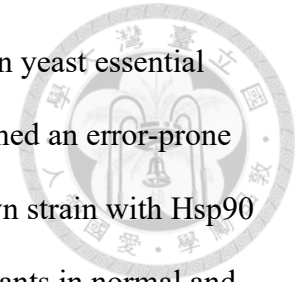
<sup>2</sup>Institute of Molecular Biology, Academia Sinica

<sup>3</sup>Institute of Information Science, Academia Sinica

## **Abstract**

Hsp90 is a molecular chaperone with a direct or indirect impact on the abundances of large portions of eukaryotic proteomes. Hsp90 has previously been observed to buffer genetic variation, meaning that its presence in the cell can nullify or reduce the strength of phenotypes associated with genetic variants or mutants. Several mechanisms have been proposed to explain this phenomenon. Some of these require that Hsp90 binds and stabilizes the mutant proteins while others posit that increases in the abundance of the protein resulting from factors downstream of Hsp90 bring that protein to a level such that it can tolerate small reductions in activity. Hsp90 bufferability may play a critical role in evolution as it decides which variants will contribute to the phenotypic diversity of a population and under which conditions. In order to assess the strength and the nature of their impact, a better understanding of the prevalence and characteristics of Hsp90-buffered variants as well as the predominant mechanism of buffering is necessary. Here, we establish

and conduct a screen for identifying Hsp90-bufferable point mutations in yeast essential genes using CBF5, a pseudouridine synthase, as the target. We transformed an error-prone PCR generated CBF5 mutant library into a CBF5 conditional knockdown strain with Hsp90 levels controlled by the Tet-Off promoter. We assayed the fitness of mutants in normal and reduced-Hsp90 conditions and identified several mutants with Hsp90-bufferable phenotypes. Furthermore, we developed an approach for rapidly identifying yeast colonies with these phenotypes based on replica plating and image analysis.

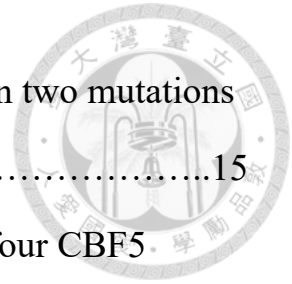


# Table of contents



<b>Certificate of thesis approval from the oral defense committee</b> .....	i
<b>Acknowledgments</b> .....	ii
<b>Mandarin abstract</b> .....	iii~iv
<b>English abstract</b> .....	v~vi
<b>Table of contents</b> .....	vii~viii
<b>Introduction</b> .....	1~7
<b>Results</b> .....	8~18
• The DDI2 promoter allows for conditional knockdown of four essential genes .....	8
• Expression level reductions of CBF5, CDC28, CDC42 and SPT15 cannot be buffered by Hsp90 .....	9
• The phenotypes of some CBF5 mutants can be buffered by Hsp90 .....	9~11
• Image analysis of replicate plates allows for more efficient identification of Hsp90-bufferable mutants .....	11~14
• Characterization of Hsp90-bufferable mutants .....	14~15





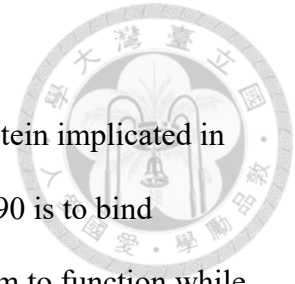
- Negative epistasis of Hsp90-bufferability between two mutations on CBF5 .....15
- No clear patterns govern Hsp90-bufferability of four CBF5 mutations .....16~18
- Discussion** .....19~23
- Materials and Methods** .....24~28
  - Yeast strains .....24
  - DDI2 insertion .....24~25
  - Library construction .....25
  - Spot assays .....26
  - Growth rate measurements .....26
  - Colony brightness measurement .....26~27
  - Site directed mutagenesis .....27
  - Extraction of yeast plasmids .....28
  - Calculation of relative solvent accessible surface area .....28
- References** .....29~32
- Figures** .....33~42
- Supplementary Figures** .....43~44
- Tables** .....45~46

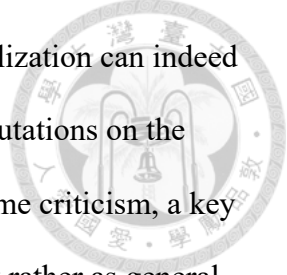
## Introduction

Hsp90 is a highly expressed and highly conserved chaperone protein implicated in the maintenance of protein homeostasis in Eukaryotes<sup>1</sup>. The role of Hsp90 is to bind unstable or misfolded proteins and hold or refold them, allowing for them to function while escaping aggregation or degradation<sup>2</sup>.

Owing to its large number of clients and the downstream effects of those clients, the activity of this chaperone exerts an enormous influence over the makeup of the proteome. In yeast, reducing the expression of Hsp90 resulted in changes in abundance of more than 20% of proteins, with approximately half of the affected proteins appearing to be Hsp90-binding clients<sup>3</sup>.

Although critical for the maintenance of cellular homeostasis on a moment to moment timescale, Hsp90 has attracted the interest of evolutionary biologists for its capacity to affect how organisms evolve over larger time periods. A genetic buffer is a system which exerts some epistatic influence over a gene or set of genes such that the correspondence between the genotype of the gene and the phenotype of the organism is obscured by the buffer<sup>4</sup>. Many systems or design schemes with extensive genetic buffering capabilities have evolved throughout life including pathways with redundant components, polyploidy and the RNAi system<sup>5,6,7,8</sup>. Genetic buffers reduce the selective constraints on the genes that they target by shielding them from the deleterious phenotypes associated with most mutations. Under some circumstances, this allows those targets to evolve new

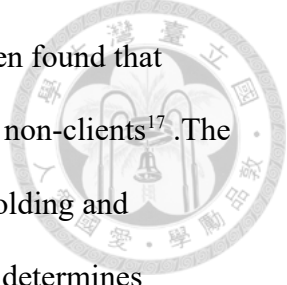




phenotypes more quickly. The well documented process of neofunctionalization can indeed be thought of as a situation in which one paralog buffers the effects of mutations on the other<sup>9</sup>. While the idea that nature selects for evolvability has received some criticism, a key insight is that these systems need not evolve as genetic buffers per se but rather as general measures to increase robustness<sup>10, 11</sup>. The same set of measures which can protect organisms from reduction in protein function brought on by changing environments and the stochasticity of intracellular processes also protect them from reductions in protein function caused by mutations.

The buildup of genetic changes and therefore variation afforded by genetic buffers allows organisms to access genotypes that may otherwise be unreachable due to phenotypic costs of intermediate steps. However, a genetic buffering system whose strength can be modulated by the environment allows not only for the buildup of genetic variation, but also for condition-specific manifestation of it as phenotypic variation. Systems with these characteristics have been dubbed ‘evolutionary capacitors’<sup>12</sup>. The existence of these systems has intrigued evolutionary biologists for their potential ability to control the level of variation, and thus the strength of natural selection in populations.

Following the pioneering work of Susan Lindquist over two decades ago, Hsp90 has been an object of interest due to its observed ability to act as an evolutionary capacitor. Reducing Hsp90 in diverse organisms such as fruit flies, arabidopsis, yeast and cavefish has been shown to exaggerate or ‘reveal’ the effects of ‘cryptic’ genetic variants that, under



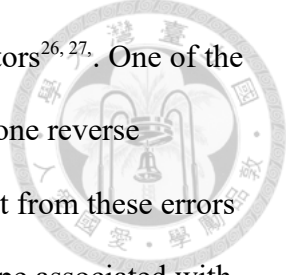
normal circumstances, are phenotypically silent<sup>12, 13, 14, 15, 16</sup>. It has also been found that kinases that are clients of Hsp90 evolve more quickly than those that are non-clients<sup>17</sup>. The most frequently cited mechanism of Hsp90's buffering effect is that by folding and stabilizing protein variants with reduced stability, the presence of Hsp90 determines whether or not mutations in proteins will result in their reduced abundance in the cell. Importantly, this explanation does not demand that the wild-type versions of the mutant proteins are themselves Hsp90 clients. It has been shown that single amino acid changes on the surface of proteins can significantly alter the dependence of those proteins' abundance on Hsp90<sup>18</sup>. This means that non-clients may be effectively turned into clients through single mutations.

Additionally, there are other possible mechanisms of buffering by Hsp90 that do not require that the mutant protein is a client of Hsp90, only that Hsp90 has some influence over the abundance of that protein (such as by stabilizing a transcription factor of that gene)<sup>19</sup>. Some phenotypes are robust to change meaning that they can be maintained in spite of perturbations in the total activity of the protein(s) linked to that phenotype. Depending on the degree of robustness, this sort of system may be able to tolerate the reduced activity/abundance associated with mutation or the reduced abundance brought on by reduced Hsp90 availability, but not both. This would result in a mutant phenotype that that only becomes apparent when available Hsp90 is reduced. Although the mechanism differs,

this indirect buffering would have the same phenotypic outcome as a mechanism involving direct stabilization of a mutant by Hsp90.

The means through which the cryptic genetic variation stored in Hsp90 buffered mutations is released is thought to be the titration of Hsp90 during protein folding stress<sup>19</sup>. According to the titration model, the number of misfolded proteins in the cell increases under stress conditions, reducing the availability of Hsp90 for any single protein. This effect has been observed and measured for several kinds of proteotoxic stress including heat stress<sup>20</sup>. This paints an intriguing picture in which stress conditions bring about phenotypic variation in populations, providing more material on which natural selection can act. Thus, Hsp90 acts as a sort of tuner for the degree of bet hedging in the population. Bet hedging provides an advantage in fluctuating environments which would likely be the same types of environments as those in which Hsp90 becomes titrated due to the cell's need to reconfigure its transcriptional program<sup>21, 22</sup>.

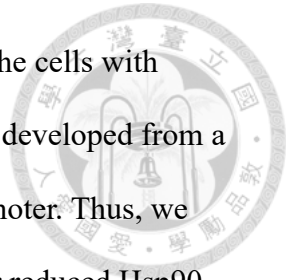
The buffering of genetic variants by Hsp90 has significant impacts on human health. Hsp90-inhibitors are a frequent target for use in cancer treatment, partly owing to the tendency of oncogenic mutant proteins to have an increased reliance on Hsp90<sup>23, 24</sup>. A classic example is provided by c-Src, a kinase which acquires oncogenic properties only after the mutation of a key regulatory residue. The resulting protein, known as v-Src has been demonstrated to have a greater reliance on Hsp90 than c-Src making it an example of an Hsp90-buffered mutant<sup>25</sup>. The buffering action of Hsp90 also plays a role in viral



infection. Viruses have been shown to be hypersensitive to Hsp90 inhibitors<sup>26, 27</sup>. One of the hypothesized reasons for this is that RNA viruses rely on highly error-prone reverse transcriptases to replicate their genomes<sup>28</sup>. The mutant proteins that result from these errors have reduced stability, requiring Hsp90 to buffer the deleterious phenotype associated with this loss of stability. Lastly, Hsp90 has been shown to modulate the severity of many mutations associated with genetic diseases in humans<sup>29</sup>.

Since an understanding of what makes some variants bufferable has considerable ramifications for both evolution and health, there has been some effort to identify the factors behind this phenomenon. A comparison of the properties of Hsp90-client kinases and non-client kinases in humans revealed key insights such as the fact that the strength of a protein's interaction with Hsp90 seems to correlate with the inherent instability of the protein<sup>30</sup>. Interestingly, it was also found that the correlation between the strength of a protein's interaction with Hsp90 and its change in abundance following Hsp90 inhibition is fairly weak.

In order to probe the properties of Hsp90-bufferable mutations even more deeply, a method with higher resolution is desirable. Even closely related members of the same protein family will differ by several amino acid positions, so it is difficult for comparisons among them to tease out which factors might contribute to bufferability and which are irrelevant. Here, we develop a screen for the investigation of the bufferability of mutants of yeast essential genes by taking advantage of error-prone PCR generated mutant libraries.



We created knockdown strains of our genes of interest and transformed the cells with plasmids harboring mutant copies of those genes. Our yeast strains were developed from a background in which Hsp90 expression is controlled by the Tet-Off promoter. Thus, we were able to measure the growth of mutants in conditions with normal or reduced Hsp90 levels by adding doxycycline to the growth media. We identified bufferable mutants as those which displayed a much larger sensitivity to Hsp90 reduction than the wild type yeast.

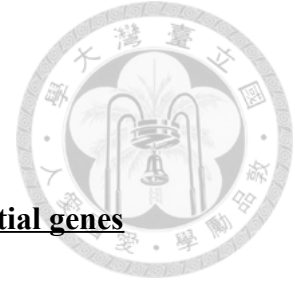
Essential genes represent ideal targets for this screen for several reasons. Their close relationship to cell survival and proliferation make it easy to evaluate their function by measuring yeast growth rate. Additionally, these genes necessarily serve important roles in the cell, so insights about their behavior will likely be useful in other contexts. So far, we have performed our screen on CBF5, an Hsp90 client which encodes a pseudouridine synthase enzyme which is necessary for stabilization of rRNA and tRNAs<sup>31,35</sup>. Currently we are preparing to screen several other genes including SPT15, another Hsp90 client which is a universal transcription factor; and CDC42, a non-client which is required for establishing cell polarity during cell division<sup>32,33,35</sup>. Our last target, CDC28 the cell cycle checkpoint mediator, has not been reported as a client of Hsp90, though its human ortholog, Cdk1 has<sup>34</sup>. By screening for Hsp90-bufferable mutations in multiple genes including clients and non-clients, we hope to assess not only the physical properties that cause some mutations to

be bufferable, but also gain some insights about the relative contributions of the different possible mechanisms of Hsp90-buffering.





## Results:

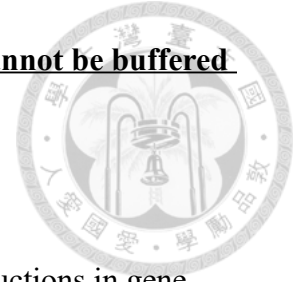


### **The DDI2 promoter allows for conditional knockdown of four essential genes**

The promoter for the gene DDI2 was previously identified as being induced by the drug cyanamide<sup>37</sup>. In order to create conditional knockdown strains for eventual screening of our mutant library, we created four yeast strains with the DDI2 promoter inserted directly upstream of our four essential genes of interest. The growth of each yeast strain was measured over time with varying concentrations of cyanamide. Our strains showed differing sensitivities to cyanamide, reflecting the different expression levels necessary to maintain their corresponding proteins at abundances sufficient for growth (Figure 1). For all strains, the difference in growth rate between growth in media without cyanamide and media with the optimal cyanamide concentration was large enough that we felt that phenotypes associated with mutants could be easily detected.

We found that for our strains, a concentration of 0.625mM allowed for growth without causing strong toxicity and thus used this condition for culturing these strains for future experiments.

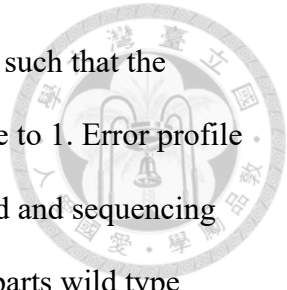
**Expression level reductions of CBF5, CDC28, CDC42 and SPT15 cannot be buffered by Hsp90**



Before our screen for Hsp90 bufferable mutants, we asked if reductions in gene expression in these four genes could themselves be buffered. To measure this, we performed spot assays with our conditional knockdown strains on YPD plates with varying concentrations of cyanamide with and without doxycycline (Figure 2). We observed that the cyanamide concentration has little effect on the response of these strains to doxycycline indicating that Hsp90 cannot buffer the effects of low expression of the four essential genes. This suggests that any mutants identified in the screen will be those that directly affect Hsp90 interaction.

**The phenotypes of some CBF5 mutants can be buffered by Hsp90**

Upon establishing conditional knockdown strains for our four genes of interest, we used error-prone PCR to generate mutant libraries for CBF5 and SPT15. Our epPCR procedure was designed to allow for mutagenesis of virtually the entire ORF of each gene. The epPCR products were then cloned into vectors containing the promoter and terminator corresponding to the gene of interest and amplified in *E. coli* (Figure 3a). We then collected *E. coli* colonies (totalling  $3.2 \times 10^9$  cells for CBF5,  $5 \times 10^{11}$  cells for SPT15) and extracted



the plasmid from the pooled samples. We calibrated our epPCR protocol such that the average number of point mutations on the genes in each library was close to 1. Error profile was checked by picking 9-10 E coli transformants, extracting the plasmid and sequencing the gene. For both genes, the libraries consisted of approximately equal parts wild type copies, single mutants and multiple mutants (Table 1).

We then transformed the CBF5 mutant library into our CBF5 conditional knockout strain (Figure 3b). To approximate the proportion of our mutant library that consists of non-functional mutants, we plated the same volume of transformants on media with and without cyanamide (Figure S1). Since cyanamide should stimulate expression of the endogenous copy of the gene and allow for the rescue of non-functional mutants, we assumed the proportion of non-functional mutants should be related to the difference in the number of colonies between the two conditions. However, we found no difference in the number of colonies between the plates. We note, however, that this methodology would fail to detect dominant negative mutants since their phenotypes would not be able to be rescued by the addition of cyanamide.

To screen mutants for Hsp90 bufferability, we measured their growth in liquid YPD media with and without doxycycline. We defined mutants as having bufferable phenotypes based on the ratio of their maximum slope in the doxycycline condition to their maximum slope in YPD. For each mutant, this ratio was normalized to that of the wild type strain. This value will henceforth be referred to as the bufferability score (Figure 4a). We defined

Hsp90 bufferable mutants as those with a bufferability score less than 0.6. In the distribution of bufferability scores, this number corresponds to the ratio at which we saw a clear separation between those mutants which appear approximately normally distributed around the wild-type bufferability of one and a second group of mutants with lower ratios (Figure 4b)

In a preliminary screen of 94 mutants, we found five with Hsp90-bufferable phenotypes. Given that our library is approximately 30% wild type, this represents 7.95% of the non-wild type, non-lethal members of our library. We note that those five colonies also have somewhat reduced growth rates even under the YPD condition. However, several colonies with low growth rates in YPD do not show a bufferable phenotype indicating that bufferability is not simply determined by basal growth rate.

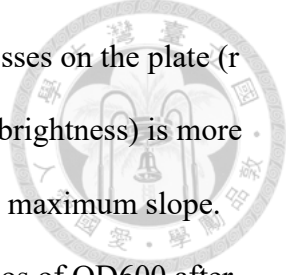
### **Image analysis of replicate plates allows for more efficient identification of Hsp90-bufferable mutants**

In order to establish a more efficient means of screening mutants, we created a script to analyze scanned images of replica plates using the Python Image Library (PIL). We transformed our mutant library to YPD plates containing its selection marker, Hygromycin B, and transferred the colonies to three other plates via replica plating. These consisted of a

YPD plate containing doxycycline, a YPD plate which would be incubated at 37°C and an additional YPD plate as a control for the efficiency of the replica process.

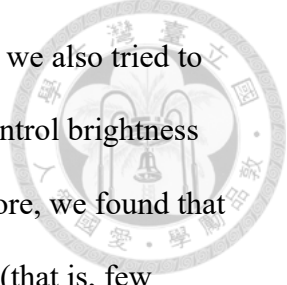
The control and 37°C plates were scanned after 1 day of growth while the replicas on the doxycycline plate were scanned after 2 days of growth. We reasoned that colonies with Hsp90-bufferable mutants should grow slower on doxycycline media and at 37°C than on YPD media at 28°C and thus appear darker in the scanned images. Thus, we wrote our script to measure the brightness of all of the colonies on each plate and for each colony, calculate the ratio of brightness on the doxycycline or 37°C plate to that on the control plate (Figure 5). We used this method to calculate these ratios for 3208 colonies across 11 initial plates of transformants. The data showed no relationship between the Dox/Ctrl ratio for a given colony and its Heat/Ctrl ratio (Figure 6). This result is surprising given that we expect Hsp90 to become titrated by misfolding proteins during heat stress. From the perspective of an individual mutant protein which requires Hsp90 to function, this effect should be similar to that of reduced Hsp90 expression brought about by doxycycline treatment. The lack of a relationship between these quantities suggests that 37°C may not have been an extreme enough condition to significantly titrate Hsp90 and thus reveal the phenotypes of Hsp90 bufferable mutants.

We then focused the imaging analysis technique on those 94 mutants previously screened in liquid culture. Of the 94, we were able to quantify colony brightness on all three plates for 84 of them. This analysis revealed a weak correlation between the



bufferability score measured from liquid culture and the ratio of brightnesses on the plate ( $r = 0.22$ ). We reasoned that for a given mutant, colony size (and therefore brightness) is more closely related to final cell density (or yield) in liquid culture than it is to maximum slope. Indeed, the correlation coefficient between ratios of brightnesses and ratios of OD600 after 36 hours is notably greater ( $r = 0.42$ ).

To test if the imaging analysis can be used to predict bufferable mutants from brightness information, we set the script to identify the 50 colonies with the lowest dox/control brightness ratios from the 3208 colonies detected. We then chose 18 predicted bufferable mutants from this set by manually inspecting the images, and used these cells for growth rate measurements in liquid culture. We compared the bufferabilities of these mutants with those of mutants selected via two other methods. The first method was picking colonies at random as discussed previously. We also tried to increase the efficiency of our screening by transforming yeast directly onto doxycycline media and picking only small colonies. A comparison of these methods showed that the imaging informed method greatly surpassed the others in terms of enriching the pool for low-bufferability score mutants (Figure 7). We caution that due to some issues we have observed with reproducibility between plate reader experiments, the comparison between the randomly picked mutants and those from transformation to doxycycline or imaging may not be apt. However, the growth rates of those mutants picked from the yeast transformed to doxycycline and those identified by imaging were measured on the same plate.

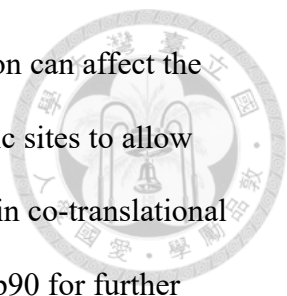


In addition to sorting the mutants by dox/control brightness ratio, we also tried to sort them by the product of their dox/control brightness ratio and heat/control brightness ratio. However, when we pulled out the top 50 colonies sorted by this score, we found that for most mutants, the product is dominated by one of the two conditions (that is, few colonies have strongly reduced growth in both conditions).

### **Characterization of Hsp90-bufferable mutants**

Through several rounds of screening (mostly using the random selection method), we identified 9 mutants with Hsp90 bufferable phenotypes that could be repeated in subsequent tests. Since it is possible that the observed phenotypes were results of mutations in the genome rather than the mutant copies of CBF5 on the plasmid, we isolated the plasmids from the 9 candidates and re-transformed them into naive yeast. The growth curves of three transformants were measured for each mutant. Although many of these mutants did not maintain a bufferability score less than 0.6, eight of them had scores that were still significantly lower than the wild type strain (Figure 8). We sequenced the copy of CBF5 in the plasmids of these mutants (Table 2). Three of the mutants had single nucleotide substitutions, four had two and one had three.

Interestingly, we observed one mutant (P1-76) which contains only a synonymous mutation. This causes a change from the less common GAG codon to the more common



GAA codon. It is currently understood that the rate of codon incorporation can affect the folding stability of proteins, with slower codons being required at specific sites to allow time for folding<sup>38</sup>. Although Hsp90 is not known to be directly involved in co-translational folding, chaperones that protect nascent polypeptides shuttle them to Hsp90 for further folding, meaning it still plays a crucial role in this process<sup>39</sup>. However, since we have not ruled out the possibility that our detection of this mutant was an experimental artifact (possibly related to changes elsewhere on the plasmid), we did not include it in further analysis.

#### **Negative epistasis of Hsp90-bufferability between two mutations on CBF5**

In mutants with multiple nucleotide substitutions, the relationship between the individual mutations and the bufferable phenotype is not clear. To address this, we used site-directed mutagenesis to recreate both component mutations of one of our mutants, P1-62 (Figure 9). While both mutations, appear to contribute some bufferability to the protein, T1036C alone appears sufficient to completely recreate the phenotype of the original double mutant. When T1036C is combined with G1356T, there is no significant change in phenotype.



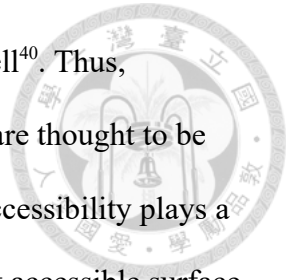
## **No clear patterns govern Hsp90 bufferability of four CBF5 mutations**



Using the two non-synonymous mutants identified by screening and the two individual mutants created by site-directed mutagenesis, we searched for features which might explain the bufferability of these mutations. While our sample of four mutations does not provide enough statistical power to make broad conclusions about Hsp90 bufferable mutations, we can nevertheless make observations about the properties of this collection of mutants.

The Blosum62 score represents the rate at which a given amino acid is found to substitute for another amino acid in nature. As amino acids with similar biochemical properties are more likely to be interchangeable, this acts as a proxy for the biochemical similarity of two amino acids with higher scores indicating higher similarity. The Blosum62 scores for the amino acid substitutions of our single mutants (2,2,1 and 0) are all 0 or greater. We generated the distribution of the Blosum62 scores of all possible non-synonymous single nucleotide mutants of CBF5 and found the median of the distribution to be 1 (Figure 10a). The medians of these two samples are significantly different (Mann-Whitney U Test:  $p = 0.00346$ ) but we note that this pattern may have arisen simply due to the fact that our bufferable mutants are necessarily non-lethal.

Since reductions in gene expression are non-bufferable, bufferable mutations should be those with increased reliance on Hsp90 for folding. Proteins generally fold to shield a



core of hydrophobic residues from the hydrophilic environment of the cell<sup>40</sup>. Thus, mutations to residues which are buried deep inside the protein structure are thought to be more destabilizing than those occurring at the surface. To determine if accessibility plays a role in the bufferability of our mutants, we calculated the relative solvent accessible surface area (RSASA) of the residues at which mutations occurred in our mutants using the crystal structure of the H/ACA ribonucleoprotein complex determined by Li et al<sup>41</sup>. Since this crystal structure does not include all residues of CBF5, this metric could not be calculated for all of the residues at which we observed mutations. The RSASAs of the three single mutants occurring at residues which are resolved in the crystal structure do not appear obviously different from what might be expected from a random sample of all of the resolved residues of CBF5 (Figure 10b).

To even more directly probe whether stability changes are the cause of the observed bufferability in our mutants, we took advantage of INPS, an online tool for predicting protein stability changes of mutants from amino acid sequences<sup>42</sup>. We chose INPS over the slightly better performing INPS-3D in order to obtain estimates for mutations affecting residues which are not included in the CBF5 crystal structure. We note that in our data, we follow the convention used by Fariselli et al. in which negative  $\Delta\Delta G$  values indicate destabilization. All four of our single amino acid variants were predicted to be slightly destabilizing ( $-1 < \Delta\Delta G < 0$ ). Since slightly destabilizing mutations represent such a large

fraction of the stability changes predicted by INPS, this information does not suggest nor rule out a relationship between stability and bufferability (Figure 10c).

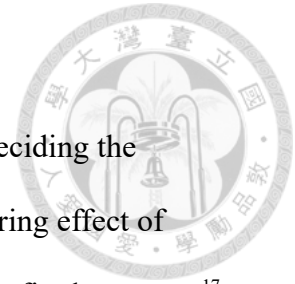


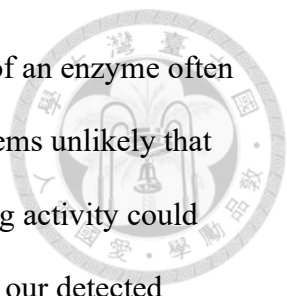
## Discussion

The Hsp90 bufferability of the mutants of a gene play a role in deciding the evolutionary future of that gene. In the case of essential genes, the buffering effect of Hsp90 opens new paths through genotypes that would otherwise cause unfit phenotypes<sup>17</sup>. Thus knowledge of the patterns underlying bufferability will allow us to predict how genotypes might change over time in a condition dependent manner.

We established a protocol for screening mutants of essential genes for Hsp90 bufferability and identified some mutations in the essential gene CBF5 with Hsp90 bufferable phenotypes. Our screen suggests that Hsp90-buffered mutants of CBF5 have a frequency of approximately 7% in our library. Further screening will be required to provide an estimate of the frequency of these types of mutations among single nucleotide mutants which should more accurately reflect the set of mutations which could realistically be sampled by evolution. Our results also suggest that for CBF5, bufferable mutants do not lack a phenotype altogether under normal conditions. Rather, the typical case appears to be that they display a phenotype that is weakly different from wild type cells but is exaggerated under conditions with reduced Hsp90. This finding is still consistent with an evolutionary capacitor model, as the absence of Hsp90 can still magnify phenotypic diversity in a population containing mutants that behave similarly to those we identified.

Our finding that reductions in expression level of our four essential genes are not Hsp90-bufferable make the relatively high frequency of bufferable mutations even more

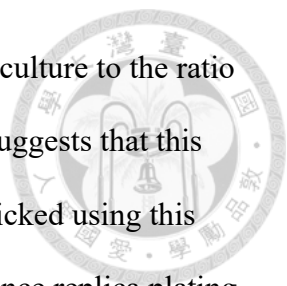




surprising. A recent paper showed that mutations in the catalytic region of an enzyme often cannot be compensated for by increased protein abundance<sup>43</sup>. Thus, it seems unlikely that the increase in abundance made possible by increased Hsp90 chaperoning activity could buffer mutations that strongly affect catalytic activity. If this is true, then our detected bufferable mutations must have some direct impact on the association between the client protein and Hsp90.

Previous studies have shown that Hsp90-bufferability correlates, albeit weakly, with protein stability<sup>30</sup>. Given this relationship, it seems reasonable to expect that bufferable mutations might be those that compromise stability. We attempted to verify this using INPS, a model created using machine learning to predict stability changes of mutants from protein sequence. This method takes advantage of factors such as hydrophobicity differences between the wild type and mutant residues as well as information about the conservation of the residues. The predicted changes in stability of our mutants were not particularly strong relative to the set of all possible mutants. This is not surprising given our small sample set and the previously mentioned weak correlation between stability and bufferability.

Due to the large number of possible mutations for any gene, it is imperative that any phenotypic screen of Hsp90 bufferability operate at a fairly high throughput in order to analyze an appreciable portion of the sample space. Here, we attempted to address this problem by creating a tool for analyzing scanned images of replica plates. The modest



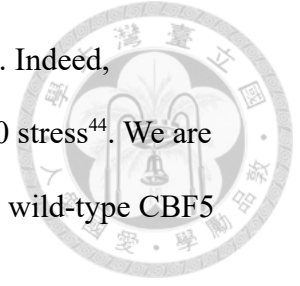
correlation ( $r = 0.24$ ) between Hsp90 bufferability as measured in liquid culture to the ratio of brightness between colonies on plates with and without doxycycline suggests that this method is somewhat informative. When the most extreme colonies are picked using this method, it massively increases the efficiency of the screening process. Since replica plating is itself a somewhat noisy and inexact method, it's possible that further refinement such as changes to the pressure we used or the initial colony size might allow us to strengthen the relationship between brightness and OD in liquid culture. Most of the mutants identified here were picked through the random selection method. We expect that the imaging aided approach will allow us to identify Hsp90 bufferable mutations in our other essential genes of interest much more quickly and identify more bufferable mutants such that we can better understand their properties.

Another high-throughput method would be to leverage a bulk-competition approach. This has the benefit of measuring phenotype more directly than imaging. We are currently planning to perform this experiment for one of our four essential genes, CDC28. This experiment will involve culturing all transformants together in liquid media and allowing them to grow for several generations. Before and after the growth period, the DNA will be collected from the yeast, the copy of CDC28 will be amplified via PCR and these amplicons will be subject to next-generation sequencing using the Illumina platform. For each mutant, the difference in its frequency in the initial population and the final population will give us information about the growth rate. By performing this experiment in media

with and without doxycycline, we can measure the Hsp90-bufferability of each mutant. Presently, we have obtained a mutant library for CDC28 which was created via semiconductor-based oligo synthesis. Due to the precision afforded by this method, we were able to obtain a library containing all possible single amino acid substitutions of CDC28 at approximately equal frequencies. This represents an improvement over epPCR-based libraries which, due to the random nature of the mutagenesis, will inevitably include non-mutants and multiple mutants.

I acknowledge that a shortcoming of our study is that mutants were classified as bufferable based on comparison of the growth profiles to those of a strain with the wild-type copy of CBF5 expressed from the genome. This design fails to account for differences in fitness or bufferability that might be brought about by the fact that the CBF5 expression in our mutants comes from a plasmid, not the genome. Indeed, when we checked the growth rates of our wild-type strain against the CBF5 conditional knockdown strain carrying the wild-type gene on the plasmid, we found that the latter responds more strongly to doxycycline, giving the wild-type gene on the plasmid itself a bufferable phenotype. The source of this phenotype is currently unknown. Since we established that gene expression reductions of CBF5 alone are non-bufferable, they should not be the cause of this discrepancy. We posit that reduction in Hsp90 level instead leads to reduced plasmid stability or asymmetric plasmid inheritance in our strains. In either case, we would expect to see a reduced growth rate in doxycycline due to the non-viability of those progeny that

do not receive a plasmid (harboring an essential gene) after cell division. Indeed, aneuploidy has previously been reported as being increased under Hsp90 stress<sup>44</sup>. We are currently checking our bufferable mutants against the strain carrying the wild-type CBF5 on a plasmid to rule out potential false positives.







## Materials and Methods

### Yeast strains

The strain used for the creation of all conditional knockdown strains in this study is derived from the BY4741 background. Additionally, our strains carry the following genetic modifications to the Hsp90 loci: hsp82 $\Delta$ ::NAT and G418-Tet-HSC82.

### DDI2 insertion

Conditional knockdown strains were generated by insertion of the DDI2 promoter between the promoter and ORF of the gene of interest. For each gene, we created a recyclable cassette in which URA3 was flanked by two identical copies of the DDI2 promoter. This sequence was in turn flanked in the 5' direction by a ~500bp region homologous to the 3' end of the promoter and in the 3' direction, a ~500bp region homologous to the start of the gene.

This design was constructed on a plasmid, excised via restriction digest and transformed into yeast using the lithium acetate method. For some inserts, we observed no transformants following this procedure. For these, we first transformed diploid cells and performed tetrad dissection on URA3 media with cyanamide to obtain haploid cells with the desired genotype. For all strains, we attempted to pop out URA3 by plating cells on 5-FOA plates containing 0.625mM Cyanamide. However, despite many attempts, we were

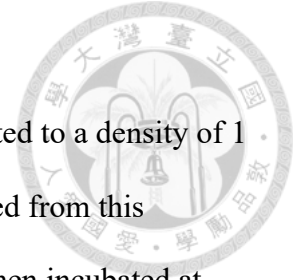
only able to successfully remove URA3 from the CDC28 conditional knockdown strain.

This indicates that changes in the leakiness of the DDI2 promoter brought on by spontaneous loss of the URA3 should not be a concern.



### **Library construction**

All plasmid construction was performed using the In-Fusion HD cloning kit from Takara Bio. The gene of interest was PCR amplified and inserted into a plasmid containing the KanR gene. This plasmid was then used as the template for error-prone PCR. epPCR was performed using the *GeneMorph II Random Mutagenesis Kit* from Agilent Technologies. For the template, we used the amount of plasmid corresponding to 1 µg of the coding sequence. The epPCR products were subsequently inserted into a vector for the expression of the gene. Our CBF5 expression vector was constructed using pRS41H as a backbone and consisted of a 480bp promoter region and 484bp terminator region separated by a *smaI* restriction enzyme cut site. The vector was linearized at this site and the epPCR product was inserted. The resulting plasmid was cloned into E coli and colonies were plated across 10 plates. After 1 day of growth, the E. coli were pooled together and the plasmid was extracted using the Presto Mini Plasmid Kit from Geneaid.



## **Spot assays**

Yeast were grown to stationary phase overnight in YPD and diluted to a density of 1 OD<sub>600</sub> in distilled water. Four 10-fold serial dilutions were then prepared from this suspension and 5 $\mu$ L of each were spotted onto agar plates. Plates were then incubated at 28°C for 3 days.

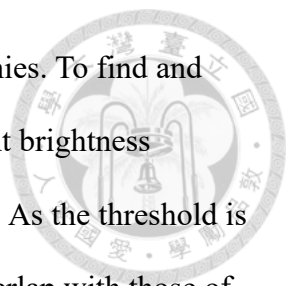
## **Growth rate measurements**

Measurements of yeast growth were performed in the Tecan Infinite 200 Pro plate reader. Following overnight culture, yeast were diluted to  $\sim$ 0.3 OD<sub>600</sub> by eye and refreshed for two hours. The absorbances of these cultures were subsequently measured and all cells were diluted to 0.1 OD<sub>600</sub> in YPD media. 60 $\mu$ L of these suspensions were mixed with 60 $\mu$ L of YPD or YPD with 0.2 $\mu$ g/mL doxycycline making the final cell density 0.05 OD<sub>600</sub> and the final doxycycline concentration 0.1 $\mu$ g/mL.

Maximum slopes were calculated by finding the 6 hour window with the greatest increase in OD<sub>600</sub>.

## **Colony brightness measurement**

Our tool for measurement of colony brightness was created in Python and took advantage of the Python imaging library. First, scanned images were aligned by adjusting the positions and rotations of the images to minimize the pixelwise difference in brightness.



Following this, the pre-replica image was used for identification of colonies. To find and count colonies of different brightnesses, the tool iterates through different brightness thresholds. Colonies are first identified as areas passing a high threshold. As the threshold is decreased, new colonies are added only if their brightest areas do not overlap with those of their neighbors. This allows for identification of dim colonies while still discriminating between neighboring colonies. The coordinates of these colonies are then mapped to the replica images and adjusted slightly to better align with the locations of the colonies on those plates. The brightness within a circle around each of these points is recorded for each plate. The radius of the circle is decided based on the mean size of colonies on the YPD plate that have no neighbors. The script outputs a table of brightnesses for all colonies on each plate, an image of each pre-replica plate with all colonies labeled and a .ppt file containing images of the top 50 colonies sorted by dox/control brightness ratios.

### **Site directed mutagenesis**

Site directed mutagenesis was performed using the QuikChange Lightning Multi Site-Directed Mutagenesis Kit from Agilent Technologies in which a mutant strand of the plasmid is synthesized from primers containing the desired nucleotide substitution and the original strand is digested by DpnI



### **Extraction of yeast plasmids**

Genomic DNA of yeast was obtained using cell lysis in a beater followed by phenol/chloroform extraction and precipitation in ethanol. The plasmid was then separated from gDNA using the Geneaid Presto Mini Plasmid Kit. The resulting plasmids were transformed into E coli for amplification.

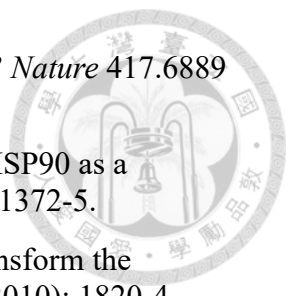
### **Calculation of relative solvent accessible surface area**


The DSSP program was used to find the accessible surface area of each residue on the CBF5 protein structure determined by Li et al<sup>41, 45</sup>. These values were then normalized to the theoretical maximum accessible surface area of each amino acid determined by Tien et al.<sup>46</sup>.

## References

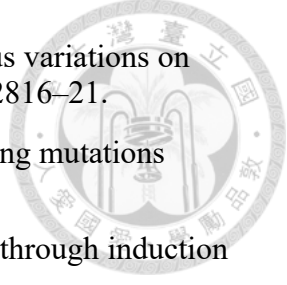


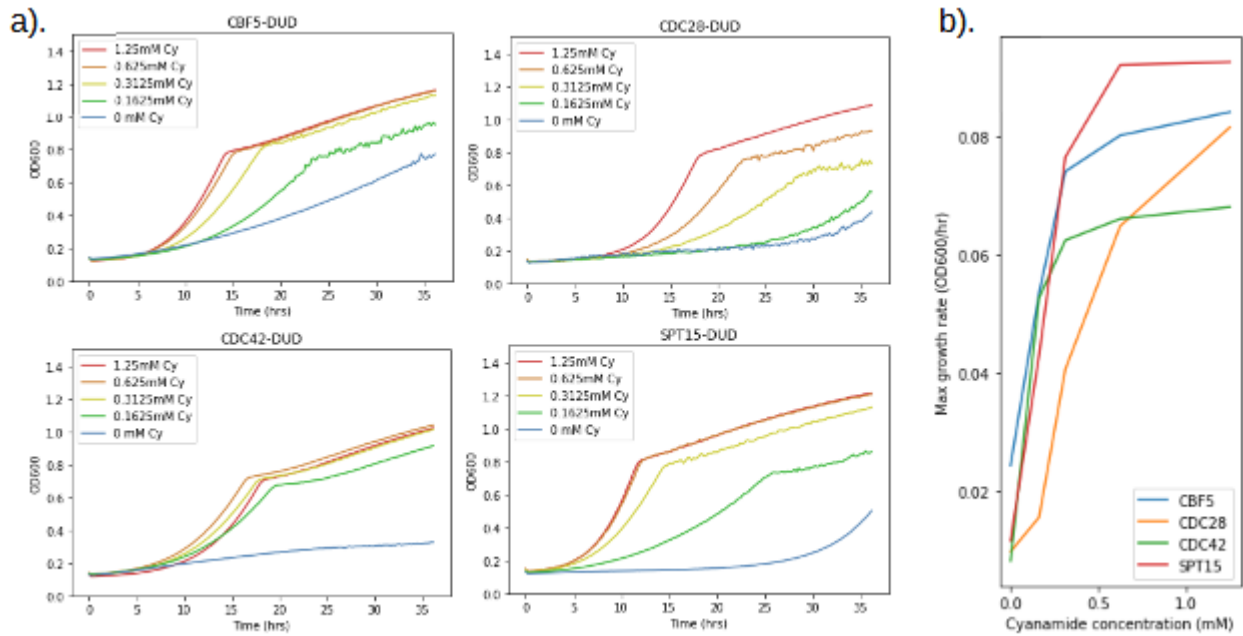
1. Borkovich KA, et al. "hsp82 is an essential protein that is required in higher concentrations for growth of cells at higher temperatures." *Mol Cell Biol.* 9.9 (1989): 3919-30
2. Schopf, F et al. "The HSP90 chaperone machinery." *Nat Rev Mol Cell Biol* 18.6 (2017): 345–360
3. Gopinath, RK et al. "The Hsp90-dependent proteome is conserved and enriched for hub proteins with high levels of protein-protein connectivity." *Genome Biol Evol.* 6.10 (2014):2851-65
4. Rutherford, SL, "From genotype to phenotype: buffering mechanisms and the storage of genetic information." *Bioessays*, 22.12 (2000): 1095-1105
5. John L. Hartman et al. "Principles for the Buffering of Genetic Variation." *Science.* 291.5506 (2001): 1001-1004
6. Van de Peer, Y et al. "The evolutionary significance of polyploidy." *Nat Rev Genet* 18.7 (2017): 411–424.
7. Conant, GC and Wagner, A. "Duplicate genes and robustness to transient gene knock-downs in *Caenorhabditis elegans*." *Proc Biol Sci.* 271.1534 (2004):89-96.
8. Lempe, J et al. "Molecular mechanisms of robustness in plants." *Curr Opin Plant Biol.* 16.1 (2013): 62-9.
9. Wang Y et al. "Genome and gene duplications and gene expression divergence: a view from plants." *Ann NY Acad Sci.* 1256.1 (2012):1-14.
10. Pigliucci, M. "Is evolvability evolvable?" *Nat Rev Genet* 9.1 (2008): 75–82.
11. Siegal, ML and Leu, JY. "On the Nature and Evolutionary Impact of Phenotypic Robustness Mechanisms." *Annu Rev Ecol Evol Syst.* 45 (2014): 496-517.
12. Rutherford, S and Lindquist, S. "Hsp90 as a capacitor for morphological evolution." *Nature* 396.6709 (1998): 336–342.
13. Sangster, TA,et al. "HSP90-buffered genetic variation is common in *Arabidopsis thaliana*." *Proc Natl Acad Sci U S A.* 105.8 (2008):2969-74.

- 
14. Queitsch, C et al. “Hsp90 as a capacitor of phenotypic variation.” *Nature* 417.6889 (2002): 618–624.
  15. Rohner, N et al. “Cryptic variation in morphological evolution: HSP90 as a capacitor for loss of eyes in cavefish.” *Science*. 342.6164 (2013):1372-5.
  16. Jarosz, DF and Lindquist, S “Hsp90 and environmental stress transform the adaptive value of natural genetic variation.” *Science*. 330.6012 (2010): 1820-4.
  17. Lachowiec, J et al. “Hsp90 promotes kinase evolution”. *Mol Biol Evol.* 32.1 (2015): 91-9.
  18. Citri, A et al. “Hsp90 recognizes a common surface on client kinases.” *J Biol Chem.* 281.20 (2006):14361-9.
  19. Sangster, TA et al. “Under cover: causes, effects and implications of Hsp90-mediated genetic capacitance.” *Bioessays.* 26.4 (2004): 348-62..
  20. Brian, D “Quantification of Hsp90 availability reveals differential coupling to the heat shock response.” *J Cell Biol* 5.11 (2018): 217.
  21. Beaumont, H et al. “Experimental evolution of bet hedging.” *Nature* 462.7269 (2009): 90–93.
  22. Gopinath, RK and Leu, JY “Hsp90 mediates the crosstalk between galactose metabolism and cell morphology pathways in yeast.” *Curr Genet.* 63.1 (2017): 23-27.
  23. Sidera, K and Patsavoudi, E “HSP90 inhibitors: current development and potential in cancer therapy.” *Recent Pat Anticancer Drug Discov.* 9.1 (2014): 1-20.
  24. Zagouri, F et al. “Hsp90 inhibitors in breast cancer: a systematic review.” *Breast* 22.5 (2013):569-78.
  25. Xu, Y and Lindquist, S “Heat-shock protein hsp90 governs the activity of pp60v-src kinase.” *Proc Natl Acad Sci U S A.* 90.15 (1993):7074-8.
  26. Connor, JH, et al. “Antiviral activity and RNA polymerase degradation following Hsp90 inhibition in a range of negative strand viruses.” *Virology.* 362.1 (2007): 109-119.
  27. Chase, G et al. “Hsp90 inhibitors reduce influenza virus replication in cell culture.” *Virology.* 377.2 (2008): 431-9.

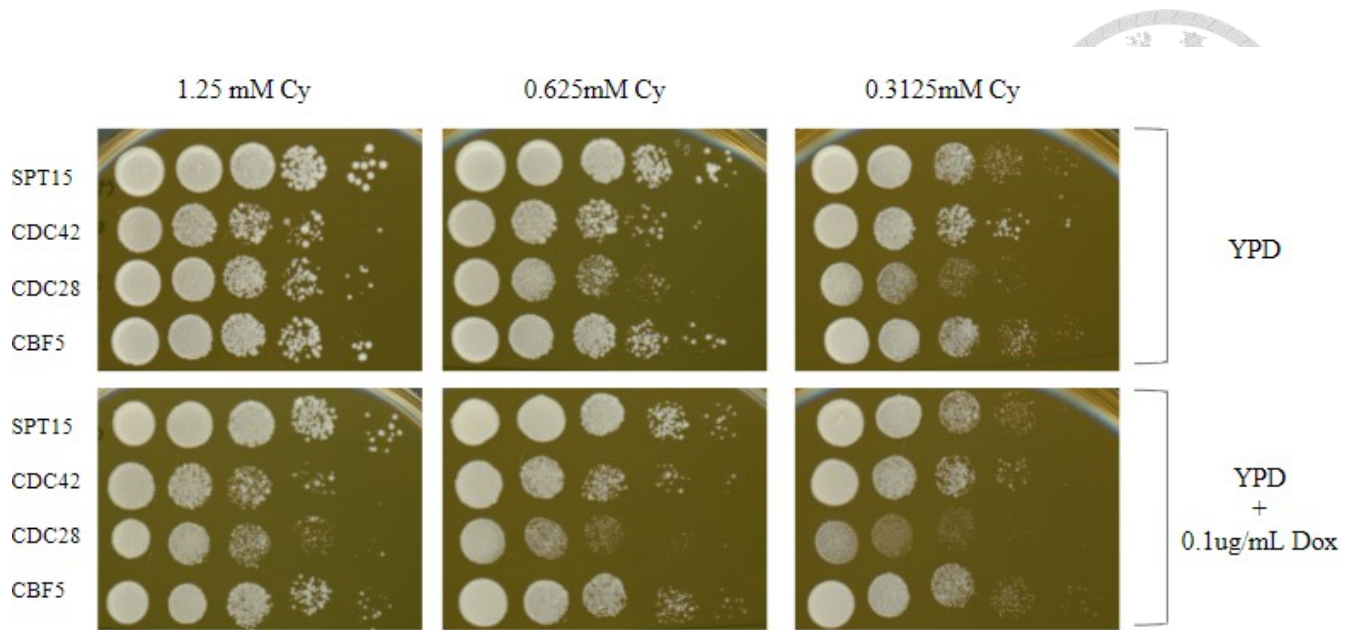
- 
28. Geller, R et al. “Broad action of Hsp90 as a host chaperone required for viral replication.” *Biochim Biophys Acta*. 1823.3 (2012): 698-706.
29. Karras, GI et al. “HSP90 Shapes the Consequences of Human Genetic Variation.” *Cell*. 168.5 (2017): 856-866.
30. Taipale, M et al. “Quantitative analysis of HSP90-client interactions reveals principles of substrate recognition.” *Cell*. 150.5 (2012): 987-1001.
31. Henras, AK et al. “Cbf5p, the putative pseudouridine synthase of H/ACA-type snoRNPs, can form a complex with Gar1p and Nop10p in absence of Nhp2p and box H/ACA snoRNAs.” *RNA*. 10.11 (2004): 1704-12.
32. Eisenmann, DM,et al. “SPT15, the gene encoding the yeast TATA binding factor TFIID, is required for normal transcription initiation in vivo.” *Cell*. 58.6: (1989): 1183-91.
33. Pruyne, D and Bretscher, A. “Polarization of cell growth in yeast. I. Establishment and maintenance of polarity states.” *J Cell Sci*. 113.3 (2000): 365-375.
34. Enserink, JM and Kolodner, RD. “An overview of Cdk1-controlled targets and processes.” *Cell Div*. 5.1. (2010): 1-41.
35. Zhao, R et al. “Navigating the chaperone network: an integrative map of physical and genetic interactions mediated by the hsp90 chaperone.” *Cell*. 120.5 (2005): 715-27
36. Caldas-Lopes, E et al. “Hsp90 inhibitor PU-H71, a multimodal inhibitor of malignancy, induces complete responses in triple-negative breast cancer models.” *Proc Natl Acad Sci U S A*. 106.20 (2009): 8368-73.
37. Wang, Y. et al. “Fine-tuning the expression of target genes using a DDI2 promoter gene switch in budding yeast.” *Sci Rep* 9.1 (2019): 12538.
38. Liu, Y. “A code within the genetic code: codon usage regulates co-translational protein folding.” *Cell Commun Signal*. 18.1 (2020): 1-19.
39. Toullec, D, et al. “The Hsp90 cochaperone TTT promotes cotranslational maturation of PIKKs prior to complex assembly.” *Cell Reports* 37.3 (2021).
40. Tokuriki, N et al. “The Stability Effects of Protein Mutations Appear to be Universally Distributed.” *J Mol Biol*. 369.5 (2007): 1318-1332.
41. Li, S et al. “Reconstitution and structural analysis of the yeast box H/ACA RNA-guided pseudouridine synthase.” *Genes Dev*. 25.22 (2011): 2409-21.



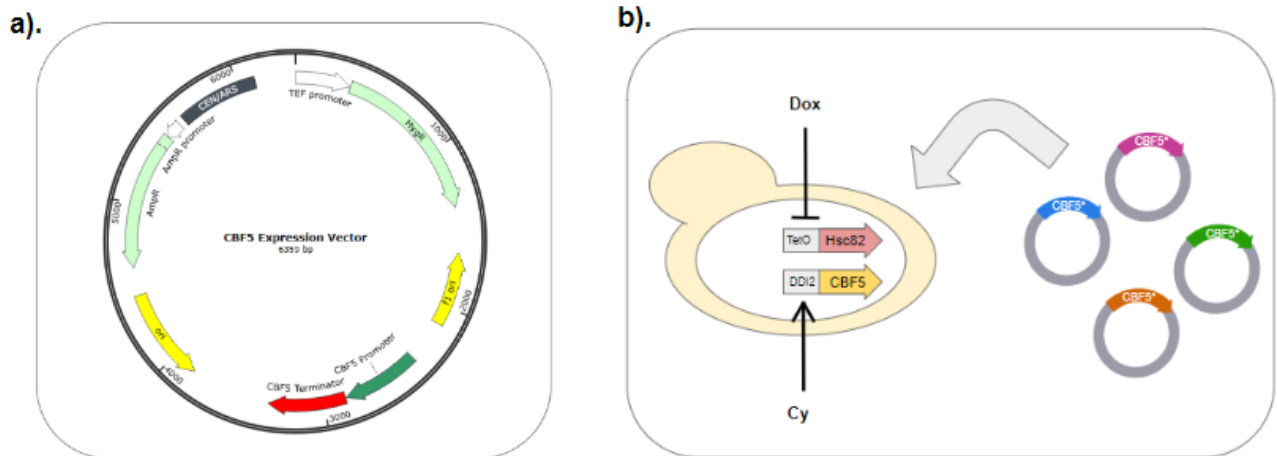
- 
42. Fariselli, P et al. “INPS: predicting the impact of non-synonymous variations on protein stability from sequence.” *Bioinformatics*. 31.17 (2015): 2816–21.
43. Cisneros, AF et al. “Epistasis between promoter activity and coding mutations shapes gene evolvability.” *Sci. Adv.* 9.5. (2013): eadd9109.
44. Chen, G et al. “Hsp90 stress potentiates rapid cellular adaptation through induction of aneuploidy.” *Nature* 482.7384 (2012): 246–250.
45. Kabsch, W and Sander, C “Dictionary of protein secondary structure: pattern recognition of hydrogen-bonded and geometrical features.” *Biopolymers* 22.12 (1983): 2577-637.
46. Tien, MZ et al. “Maximum allowed solvent accessibilities of residues in proteins.” *PLoS One*. 8.11 (2013): e80635.



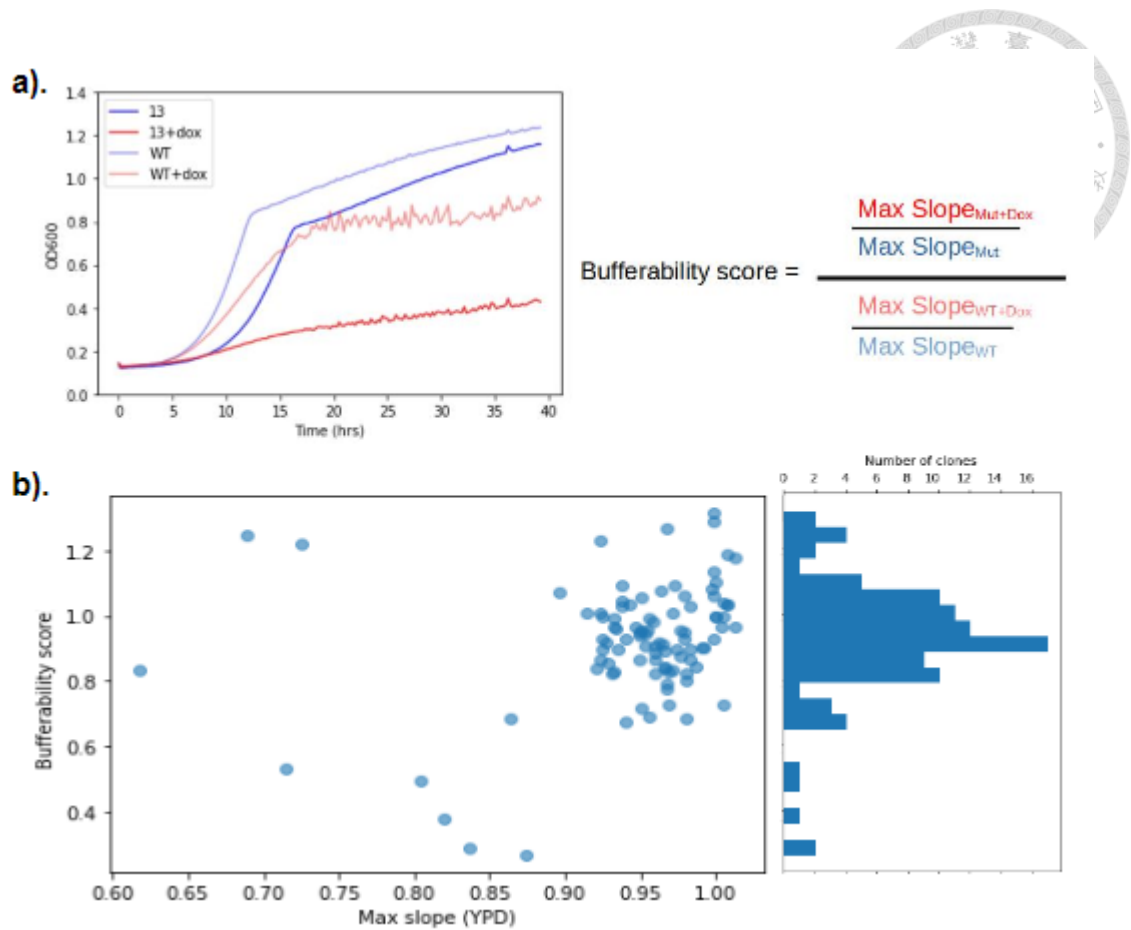
**Figure 1).** Cyanamide response data for conditional knockdown strains. **a).** Growth curves of different strains in the presence of varying doses of cyanamide. **b).** Effect of cyanamide dose on maximum growth rate for each strain



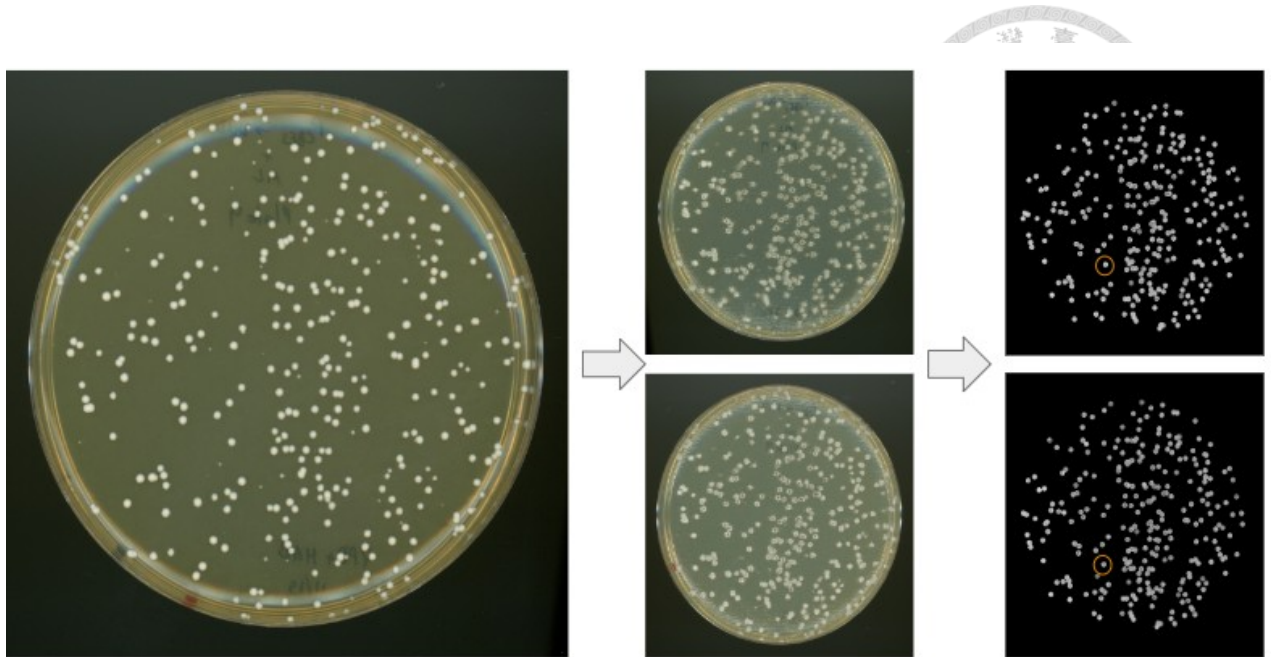
**Figure 2).** Spot assays for conditional knockout strains on varying concentrations of cyanamide with and without doxycycline. Reduced expression level does not appear to increase sensitivity to Hsp90 inhibition.



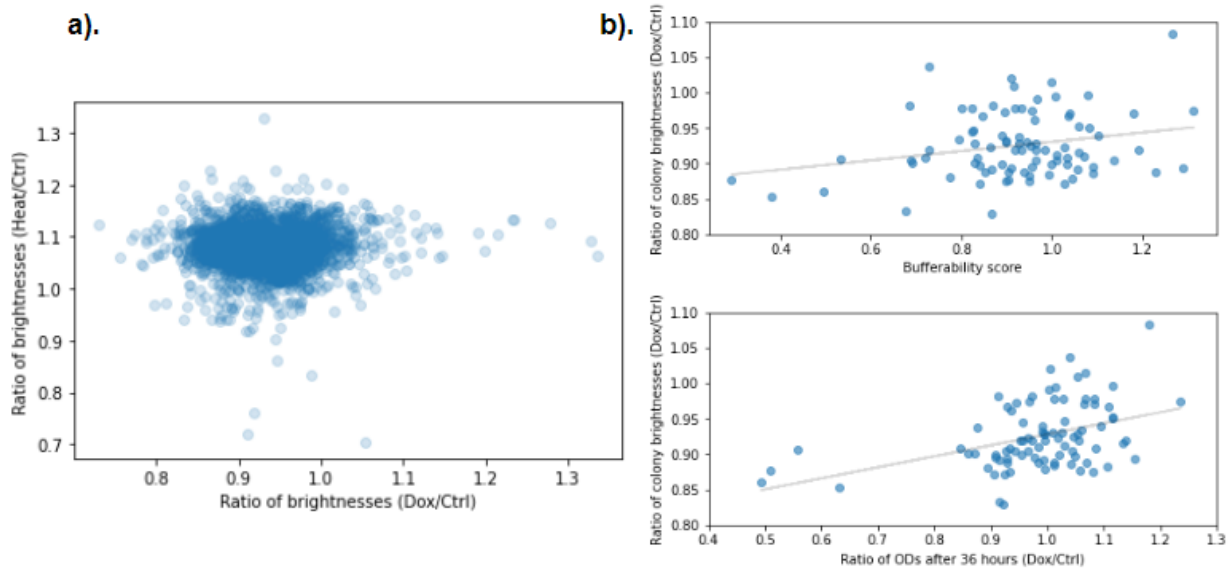
**Figure 3).** Experimental design. **a).** Design of the vector used for expression of the mutant library. Promoter and terminator are separated by a cut site for *sma*I. The plasmid is digested by *sma*I and error-prone PCR products are cloned into the construct. **b).** Experimental setup and relevant genotypes of our yeast strain. DDI2 allows for the expression of CBF5 prior to transformation with the mutant library. Following transformation, cells are cultured without cyanamide linking their phenotype only to the mutant copy.



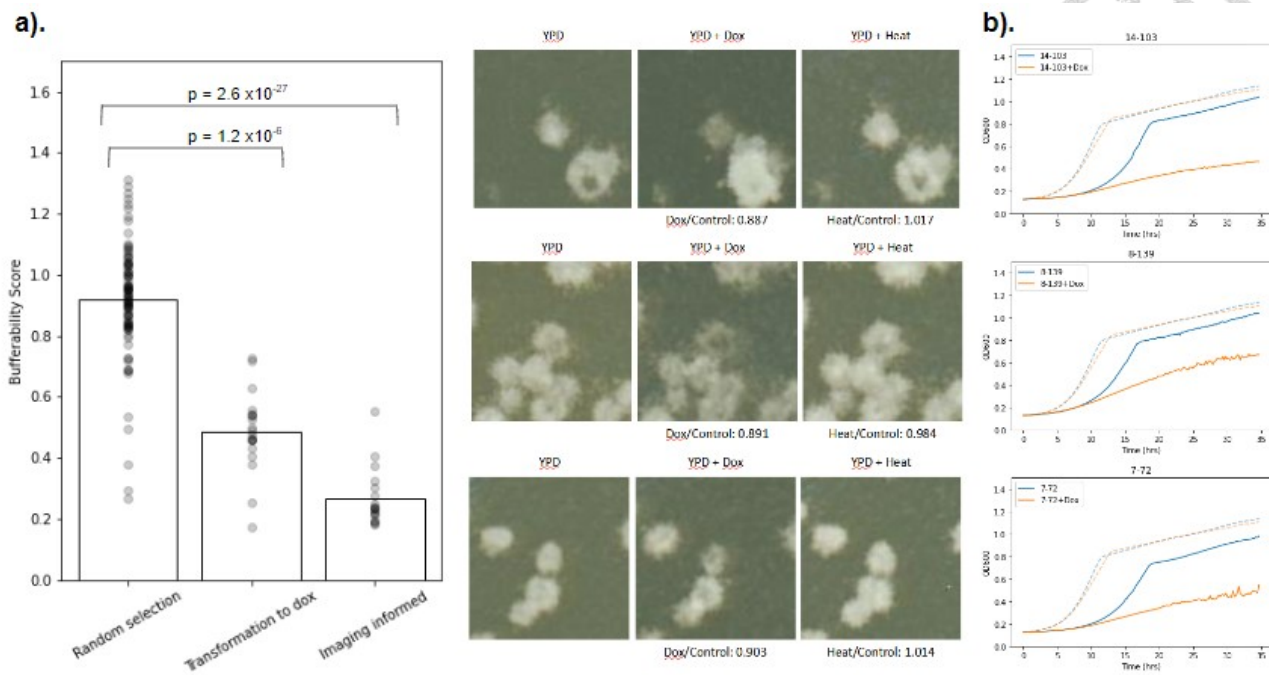
**Figure 4a).** Growth rate data from a bufferable mutant and the definition of bufferability score used in this study. Low score indicates more bufferable. **b).** Relationship between bufferability and maximum slope (normalized to that of WT). All bufferable mutants have a reduced growth rate, but not all slow growing mutants display bufferability. The histogram of bufferability shows a region which resembles symmetric variation around the wild type level but also a set of mutants with much lower values around 0.4.



**Figure 5).** General overview of imaging method. The plate is scanned before replication, then replicated to YPD, doxycycline and heated plates. The location of each colony is determined from the pre-replication image and used as the center point for circles which will be used to measure brightness.

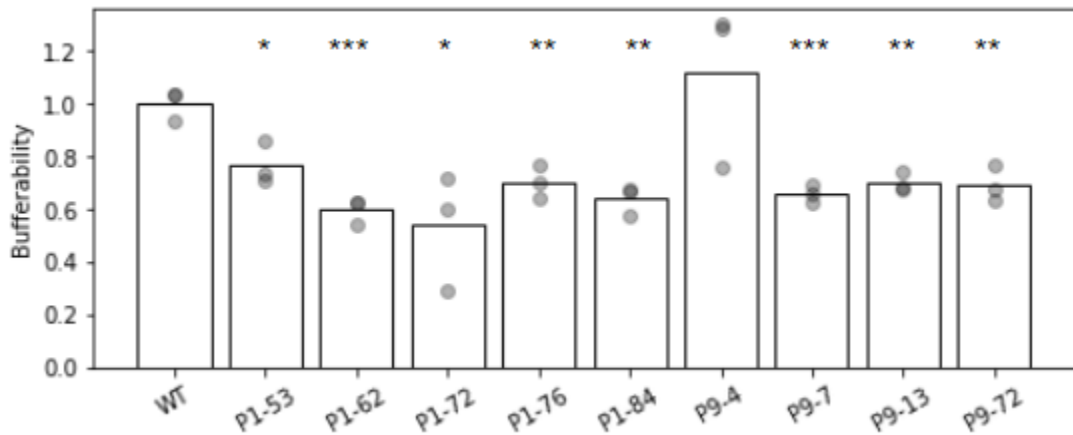


**Figure 6a).** No clear correspondence between the colonies that grow poorly in doxycycline and those that grow poorly at 37°C. **b).** Weak correlation between brightness ratios and metrics measured in liquid culture. Ratios of cell densities after 36 hours correlated more closely with colony brightnesses than did ratios of maximum slopes



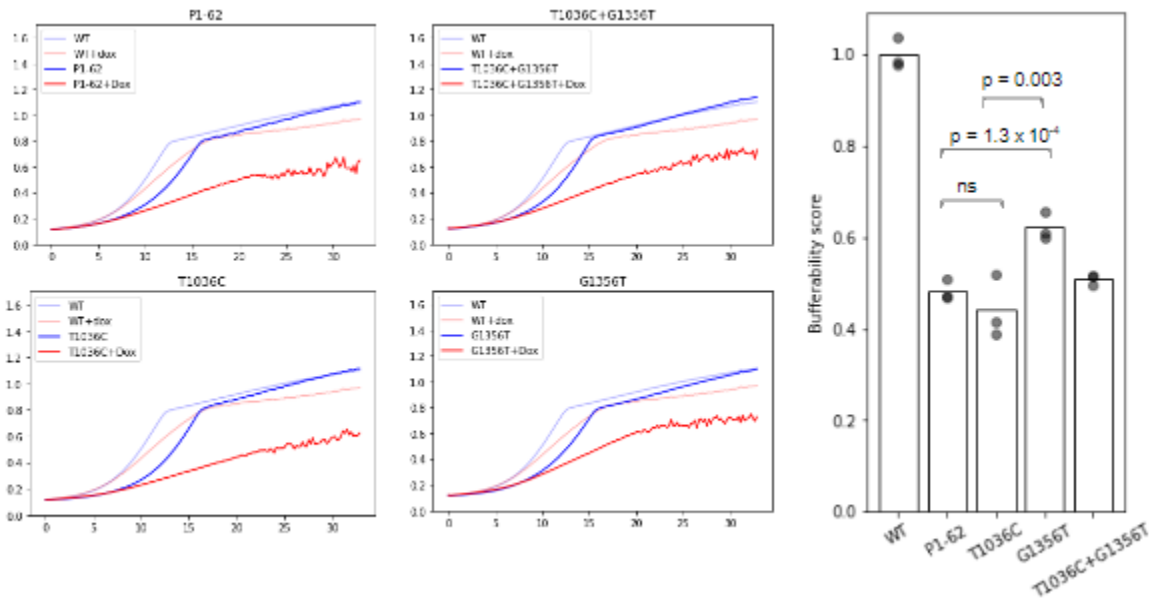
**Figure 7a).** Comparison of the bufferability of colonies picked via 3 methods. Random choice, selection of small colonies following transformation to doxycycline and those selected from the list of mutants with the smallest Dox/YPD brightness ratios. **b).** Pictures of some representative colonies from the sorted list and their growth profiles in liquid culture.



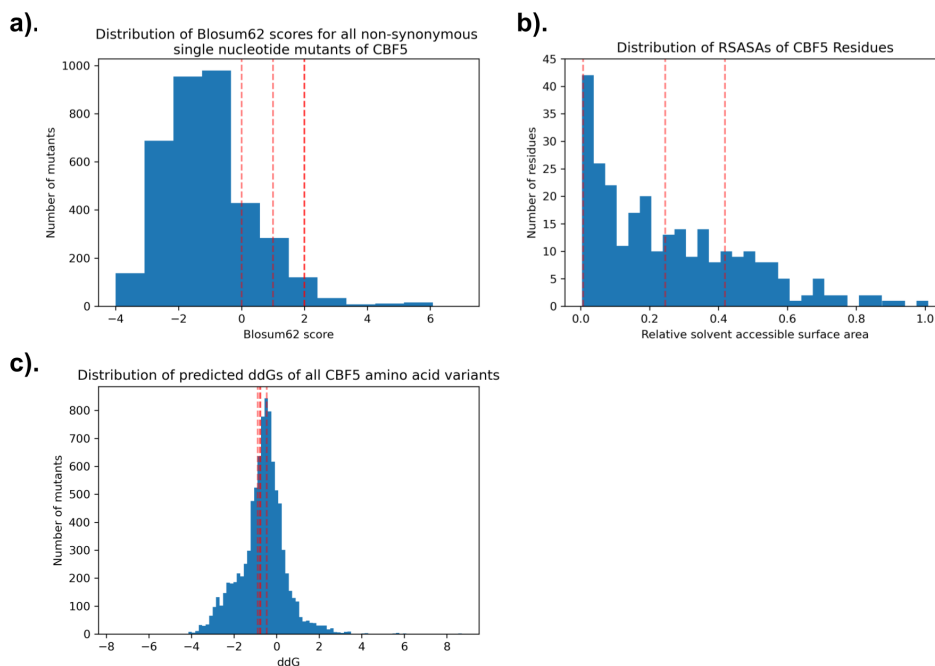


**Figure 8).** Measurement of bufferability score upon plasmid extraction and re-transformation. Points represent biological replicates. Transformants with all but one plasmid had bufferability scores significantly different from the wild type.

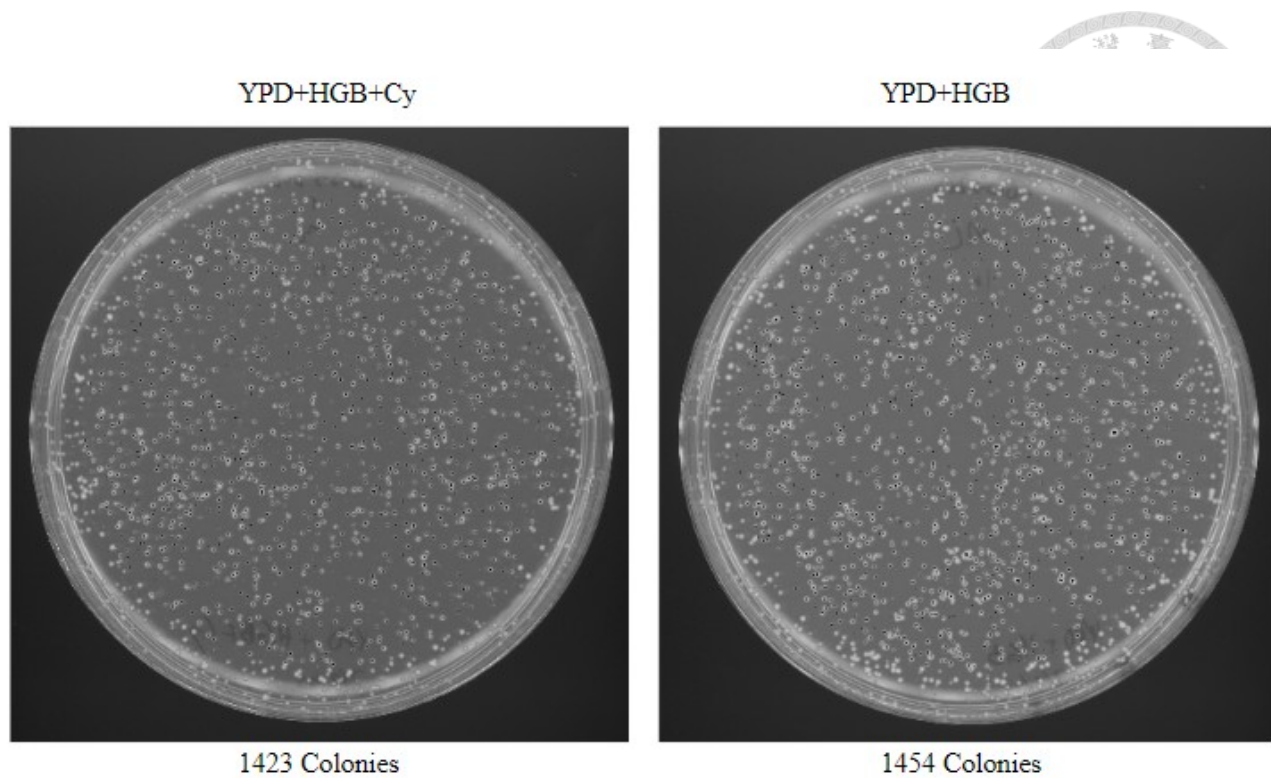
- \*  $p < 0.05$
- \*\*  $p < 0.01$
- \*\*\*  $p < 0.001$



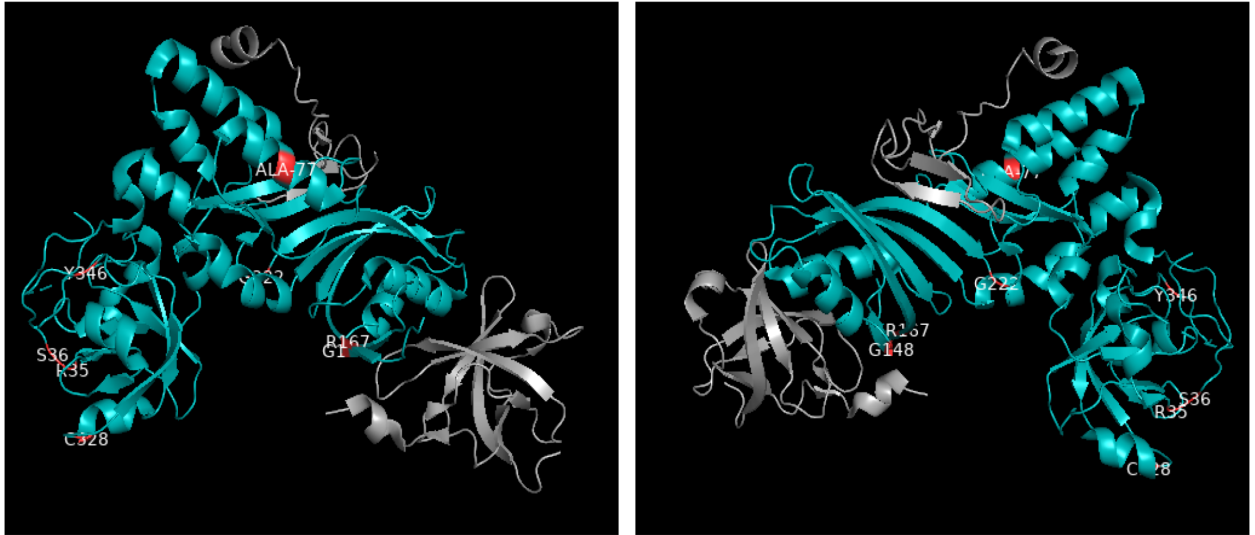
**Figure 9).** Negative epistasis of buffered mutations. Both T1036C and G1356T increase bufferability alone, but their effects do not add.



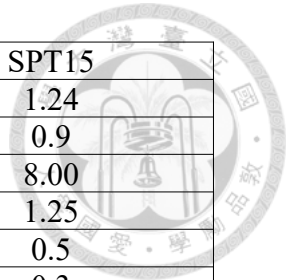
**Figure 10).** Features of the bufferable CBF5 mutants. **a).** Our four mutants (red dotted lines) have Blosum62 scores significantly higher than the median of the distribution of all scores for all possible CBF5 single nucleotide variants. (Mann-Whitney U Test:  $p = 0.00346$ ) **b).** The distribution of relative solvent accessible surface areas of the residues mutated in our single mutants compared to all residues in the CBF5 crystal structure. **c).** The predicted  $\Delta\Delta G$  scores of our mutants compared with the distribution of those of all possible CBF5 amino acid variants



**Figure S1).** Colony counts in the CBF5 conditional knockout strain transformed with the mutant library. Colonies counted using a python script. Contiguous black areas indicate regions counted as single colonies. The similar colony number indicates that non-functional CBF5 mutants are either rare or mostly dominant negative.

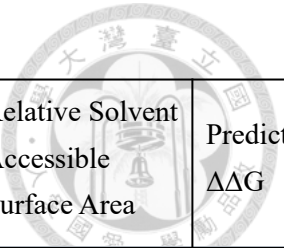


**Figure S2).** Locations of all resolved residues found to be mutated in bufferable mutants.



	CBF5	SPT15
Mean Mutations/Kb	0.92	1.24
Mean Mutations/Gene	1.33	0.9
Transitions/Transversions	1.00	8.00
Sites: (AT/GC)	0.71	1.25
Fraction Wild type	0.33	0.5
Fraction Single Mutants	0.33	0.3
Fraction Multiple Mutants	0.33	0.2

**Table 1).** Test libraries of mutant libraries for CBF5 and SPT15. Obtained by randomly picking colonies of *E. coli* transformed with the library



Mutant	Bufferability score	Nucleotide change	Amino acid change	BLOSUM62 score	Relative Solvent Accessible Surface Area	Predicted $\Delta\Delta G$
P1-53	0.766	G104A	R35K	2	0.245	-0.887325
P1-62	0.598	T1036C G1356T	Y346H K453N	2 0	0.007 -	-0.7616135 -0.787778
P1-72	0.538	G229T	A77S	1	0.419	-0.4647635
P1-76	0.703	G1224A	E409E	5	-	0
P1-84	0.638	G442A G500T G1118A	G148S R167L R373H	0 -2 0	0.25 0.208 -	-0.895519 0.0835478 -0.683844
P9-7	0.659	G562A T982G	A188T C328G	0 -3	- 0.204	-0.46379225 -2.31423
P9-13	0.699	A106T G1080A	S36C K361K	-1 5	0.194 -	-0.290445 0
P9-72	0.692	T311C G665A	V104A G222D	0 -2	- 0.173	-2.52339 -0.914077

**Table 2).** Characterization of bufferable mutants. Shaded rows represent those mutations that have been tested individually.